Biosensors and Bioelectronics 48 (2013) 56–60

Contents lists available at SciVerse ScienceDirect

Biosensors and Bioelectronics

journal homepage: www.elsevier.com/locate/bios

Perovskite $LaTiO_3$–Ag0.2 nanomaterials for nonenzymatic glucose sensor with high performance

Yin-zhu Wang [a,b], Hui Zhong [a,b,*], Xiao-mo Li [a], Fei-fei Jia [a], Yi-xiang Shi [a], Wei-guang Zhang [a], Zhi-peng Cheng [a], Li-li Zhang [a], Ji-kui Wang [b]

[a] Jiangsu Key Laboratory for Chemistry of Low-Dimensional Materials, School of Chemistry & Chemical Engineering, Huaiyin Normal University, Huaian 223300, PR China
[b] College of Sciences, Nanjing University of Technology, Nanjing 210009, PR China

ARTICLE INFO

Article history:
Received 31 December 2012
Received in revised form
7 March 2013
Accepted 27 March 2013
Available online 11 April 2013

Keywords:
Nonenzymatic electrocatalytic oxidation
Glucose perovskite $LaTiO_3$–Ag0.2

ABSTRACT

In this paper, a nonenzymatic glucose biosensor based on perovskite $LaTiO_3$–Ag0.2(LTA) modified electrode was presented. The morphology and the composition of the perovskite $LaTiO_3$–Ag0.2 nanomaterials were characterized by using scanning electron microscopy (SEM) and X-ray diffraction (XRD) respectively. The $LaTiO_3$–Ag0.2(LTA) composite was investigated by electrochemical characterization using cyclic voltammetry (CV) and electrochemical impedance spectroscopy (EIS). Under optimal conditions, CV and chronoamperometry (I-t) study revealed that, compared with the bare glassy carbon electrode (GCE), the modified electrode showed a remarkable increase in the efficiency of the electrocatalytic oxidation of glucose, starting at around +0.70 V (vs. Ag/AgCl). The prepared sensor exhibited a high sensitivity of 784.14 $\mu AmM^{-1}\ cm^{-2}$, a low detection limit of 2.1×10^{-7} M and a wide linear range from 2.5 μM to 4 mM ($R=0.9997$). More importantly, the LTA modified electrode was also relatively insensitive to commonly interfering species such as ascorbic acid (AA), uric acid (UA), dopamine (DA) in high potential. Moreover, the nonenzymatic sensor was applied to the determination of glucose in human serum samples and the results were in good agreement with clinical data. Electrodes modified with perovskite nanomaterials are highly promising for nonenzymatic electrochemical detection of glucose because of their high sensitivity, fast response, excellent stability and good reproducibility.

1. Introduction

Glucose detection is essential in clinical diagnostics, biotechnology and food industry (Lu et al., 2012). Since enzyme electrode was revealed for detecting glucose in 1962 (Clark and Lyons, 1962), glucose sensors have received great attention in the following decades. The amperometric glucose sensor is one of the most promising techniques among multifarious glucose measuring methodologies, in which the enzyme glucose oxidase (GODx) is used as the momentous constituent to catalyze the oxidation of glucose to gluconolactone (Pang et al., 2010). However, the enzymatic sensor is short of long-term stability due to the intrinsic features of enzymes, whose activity can be easily affected by temperature, pH value, humidity, and toxic chemicals (Wilson and Turner, 1992). To overcome this obstacle, studies have been carried out to prepare nonenzymatic sensors based on the direct oxidation of glucose for extended usage.

For the fabrication of nonenzymatic biosensors, the promotion of analytical performance (e.g., sensitivity, selectivity and durability) relies more and more on the modified material (Zhu et al., 2008).With the development of nanostructured materials and nanotechnology in the area of medicine and biotechnology, nanosized particles have been gradually applied to nonenzymatic glucose sensors for their remarkable physical and chemical properties (Lin et al., 2010). For example, NiO–Au hybrid nanobelts (Ding et al., 2011), CuS nanotubes (Lu et al., 2009), CuO nanoparticles-modified carbon nanotube (Jiang and Zhang, 2010) and palladium nanoparticle-graphene nanohybrids (Lu et al., 2011) have all shown good electrocatalytic activities toward the oxidation of glucose.

Currently, inorganic perovskite type nanomaterials, whose structure can accommodate most of the metallic ions in the periodic table with a significant number of different anions, have been brought into the fields of chemically modified electrodes. Some of their properties such as photocatalytic property, conductivity and thermoelectric properties have been widely investigated (Ye et al., 2012). Up to now, only several perovskite-type composite

* Corresponding author at: Jiangsu Key Laboratory for Chemistry of Low-Dimensional Materials, School of Chemistry & Chemical Engineering, Huaiyin Normal University, Huaian 223300, PR China. Tel.: +8613952328084.
E-mail addresses: huizhong@hytc.edu.cn, huizhong96@126.com (H. Zhong), wjk@njut.edu.cn (J.-k. Wang).

0956-5663/$ - see front matter © 2013 Elsevier B.V. All rights reserved.
http://dx.doi.org/10.1016/j.bios.2013.03.081

oxides, such as $LaNi_{0.5}Ti_{0.5}O_3$ (Wang et al., 2010), $LaNi_{0.6}Co_{0.4}O_3$ nanocomposites (Zhang et al., 2012) and $LaNiO_3$ perovskite-type oxide nanofibers (Wang et al., 2013), have been proposed to improve the performance of nonenzymatic glucose sensors. It is clear that novel functional materials are needed to develop effective enzyme-less glucose sensors.

Silver exhibits excellent electrical conductivity and silver nanoparticles (AgNPs) have been traditionally explored as catalysts in various reactions (Zhu et al., 2005). Herein, we construct a glucose electrochemical sensor based on perovskite $LaTiO_3$–Ag0.2 (LTA) modified gassy carbon electrode (GCE). The electrooxidation of glucose at the prepared modified electrode was studied by cyclic voltammetry and chronoamperometry in the NaOH solution. The mechanism of the reaction was considered to involve the dehydrogenation reaction between AgO and glucose, with the oxidation current appearing in the cathodic scan due to the reoxidation of silver(I) to silver(II). Meanwhile, the application of this sensor for determining glucose concentration of human serum sample confirms its high sensitivity and accuracy. Therefore, with good analytical performance, simple preparation and low cost, these LTA nanoparticles are promising for nonenzymatic glucose sensing.

2. Experimental

2.1. Reagents and chemicals

D-(+)-Glucose, KH_2PO_4, L-Asorbic (AA), Dopamine Hydrochloride (DA), Uric acid (UA) were purchased from Sinopharm Group Chemical Reagent Co., Ltd., Shanghai, China. NaOH were obtained from Nanjing chemical Reagent Co., Nanjing, China. All chemicals and reagents used in this work were of analytical grade and used as received without further purification. All solutions were prepared with double distilled water. NaOH (0.2 M) solution was chosen as the supporting electrolyte.

2.2. Synthesis of $LaTiO_3$–Ag0.2 perovskite nanomaterials

Perovskite type $LaTiO_3$–Ag0.2 was prepared by a particulate sol–gel method (Sumio et al., 2004; Bohnke et al., 2001). $AgNO_3$, $La(NO_3)\cdot 6H_2O$ and butyl titanate were dissolved in anhydrous ethanol. The contents were stirred and the mixture of butyl titanate with concentrated nitric acid was added drop-wise until the contents became uniform. The solution was stirred with a magnetic stirrer for 10 min to ensure that the $La(NO_3)_3$ and $AgNO_3$ are completely dissolved. Under constant stirring, butyl titanate was dropped into the $La(NO_3)_3$ and $AgNO_3$ solution at room temperature. The molar ratio among $La(NO_3)\cdot 6H_2O$, $AgNO_3$ and butyl titanate was 0.8:0.2:1 and the molar ratio among anhydrous ethanol, butyl titanate and concentrated nitric acid was 120: 20: 1. When the reaction was stopped, the contents were stabilized at 7 °C until sol–gels were formed. Subsequently, the above solution was transformed into a Teflon-lined stainless steel autoclave (50 mL capacity), maintained at 180 °C for 24 h and cooled to room temperature naturally. After filtration and washing, the residue was dried and calcined in a muffle furnace at 800 °C for 6 h.

2.3. Characterization

The microstructures of the samples were characterized by scanning electron microscopy (SEM) (JSM-6380LV, JEOL, Japan). The crystal structures of the samples were examined by an X-ray diffractometer (XRD, BrukerD8, Advanee, Germany) with Cu Kα radiation (λ) 0.15406 nm.

2.4. Electrochemical measurements

Electrochemical impedance spectroscopy (EIS) measurements were performed with an Autolab PGSTAT 30 analyzer (Metrohm Autolab B.V., Switzerland). The cyclic voltammetry (CV) and amperometry were executed on a CHI660D electrochemical workstation (Shanghai Chenhua Instrument Co. Ltd., China) with a traditional three-electrode system composed of a perovskite LTA modified GCE, an Ag/AgCl (saturated KCl) reference electrode and a platinum wire counter electrode. Amperometric measurements were carried out in NaOH solution under continuous stirring. All electrochemical measurements were conducted at room temperature.

2.5. Electrodes preparation and modification

3 mg of perovskite material LTA was firstly added to 1 mL double distilled water to form a homogeneous dispersion with mild ultrasonication. Then, 5 μL of the homogeneous suspension was spread evenly onto the well-polished GCE surface with a syringe and allowed to dry in ambient air for 24 h to prepare a LTA modified GCE. The electrode was washed by double distilled water and stored at room temperature when not in use.

2.6. Procedure

EIS studies of bare and LTA modified GCEs were performed in 0.1 M KCl solution containing 5 mM $K_3Fe(CN)_6/K_4Fe(CN)_6$ by using an alternating current voltage of 10 mV, and the measurements were recorded at a bias potential of 200 mV within a frequency range of 10^{-1}~10^5 Hz. The cyclic voltammetry studies for bare and LTA modified GCEs were performed in 0.1 M KCl solution containing 5 mM $K_3Fe(CN)_6/K_4Fe(CN)_6$ and in 0.2 M NaOH solution containing 1.0 mM glucose with a scan rate of 100 mV/s. Amperometric curves were obtained after adding a glucose solution of certain concentration into the NaOH electrolyte under stirring conditions, and then the current in each experiment was recorded when it reached the steady state.

3. Results and discussion

3.1. Characterization of $LaTiO_3$–Ag0.2

XRD and SEM were used to characterize the phase structure and morphology of the $LaTiO_3$–Ag0.2, respectively. Fig. 1A shows XRD characterization of $LaTiO_3$–Ag0.2. It can be seen that the obtained $LaTiO_3$–Ag0.2 has two species at least, including $LaTiO_3$ and Ag. The peaks at 2 around 22.78°, 32.54°, 40.18°, 46.80°, 52.60°, 58.14°, 68.27°, 73.1° and 77.70° illustrate that $LaTiO_3$ keeps a face-centered cubic (fcc) structure, but diffraction peak moves to lower angle position, which is probably due to the unit cell expansion by addition of Ag. Fig. 1 shows the SEM image of $LaTiO_3$–Ag0.2. Much irregular Ag powders adhere to the surface of the spherical $LaTiO_3$ particles before the doped Ag (I) substitutes the La (III) of A-site to maintain the charge balance. This observation agrees with the structure analysis from the XRD pattern.

3.2. Electrochemical characterization of LTA modified GCE

The whole process of the preparation of modified electrodes was monitored by EIS. This can give useful information about the impedance changes on the electrode surface between each step (Gu et al., 2001). In electrochemical impedance spectroscopy measurements, the semicircle diameter of EIS is equal to that of the electron transfer resistance (Ret), which controls the electron-transfer kinetics of the redox probe at the electrode interface and

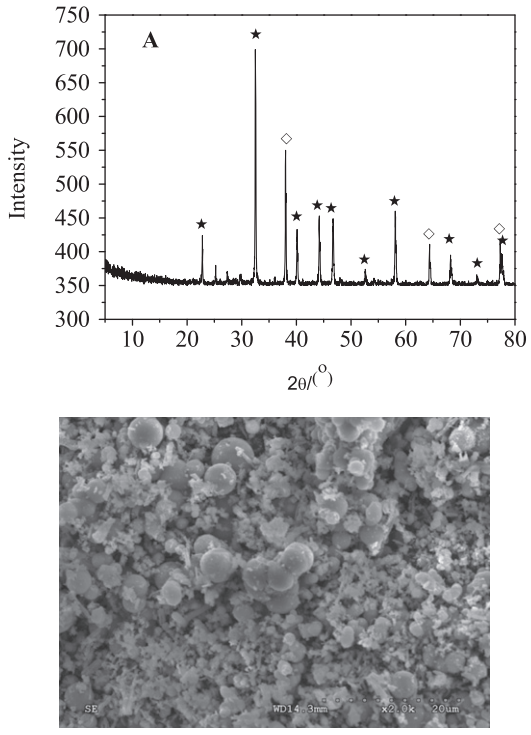

Fig. 1. XRD characterization of the $LaTiO_3$–Ag0.2 (★ $LaTiO_3$ ◇Ag) (A) and the SEM images of the LaTiO3–Ag0.2. (B).

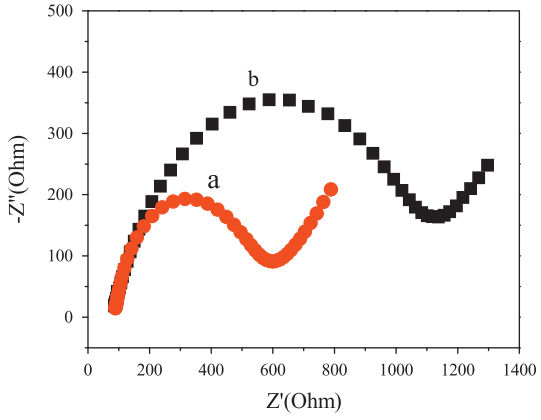

Fig. 2. Nyquist plots of GCE (a) and LTA/GCE (b) in 0.1 M KCl solution containing 5 mM $[Fe(CN)_6]^{3-/4-}$.The frequency range was from 0.1 to 1×10^5 Hz.

is an important parameter. Fig. 2. exhibits the representative impedance spectrum of the bare GCE, LTA-GCE in 5.0 mM $K_3[Fe(CN)_6]/K_4[Fe(CN)_6]$ (1:1) containing 0.1 M KCl. The Nyquist semicircle of the LTA/GCE (curve b) increased dramatically compared with the bare GCE (curve a), indicating that LTA with semiconductive nature of perovskite has formed an effective film on the surface of GCE, which weakened the electroconductivity of the electrode.

3.3. Electrochemical behavior of glucose on the LTA/GCE

In order to test the electrocatalytic activity of the synthesized LTA catalyst toward glucose oxidation, typical cyclic voltammograms were obtained at bare and LTA modified GCE in 0.2 M NaOH solution without and with 1.0 mM glucose, respectively, at a scan rate of 50 mV s^{-1} as shown in Fig. 3.A. No redox peaks were observed for cyclic voltammograms at the bare GCE in the range of 0.10~0.90 V in the NaOH solution without (a) and with (b) glucose,

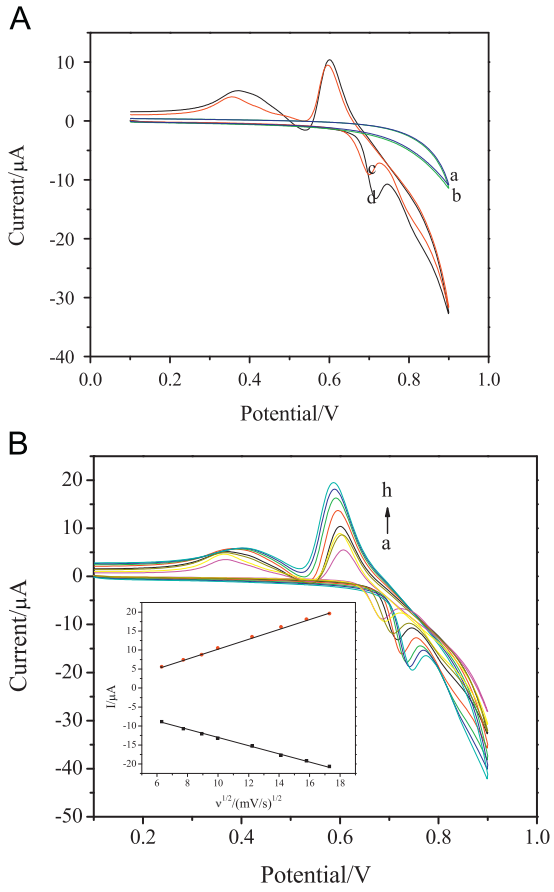

Fig. 3. Cyclic voltammograms of bare GCE (a,b) and LTA/GCE (c,d) modified electrode in the absence (a,c) and presence (b,d) of 1.0 mM glucose in 0.2 M NaOH at scan rate of 0.1 V/s (A). Effect of the scan rate on the anodic peak current (1.0 mM glucose in 0.2 M NaOH). Inset: The square root of the scan rates (B).

suggesting that bare GCE does not have any electrocatalytic activity toward the oxidation of glucose within this range. While for the LTA/GCE, during the forward scan, a sharp anodic peak was observed at around 0.70 V, and in the reverse scan, two cathodic peaks appeared at 0.61 and 0.32 V respectively in the blank NaOH solution (c). This means that the LTA modified GC electrode exhibits characteristic and larger catalytic response than bare GCE.

According to previous reports(Gu et al., 2001; DeMott and Jahngen, 2005) the anodic peak (0.70 V) is attributed to the oxidation of Ag_2O to AgO or direct oxidation of Ag to AgO. The cathodic current peak (0.61 V) is due to the reduction of AgO to Ag_2O, and the cathodic current peak (0.32 V) can be ascribed to the reduction of Ag_2O to Ag. Upon the addition of glucose, a distinct enhancement of the anodic current was observed (*d*), representing pronounced glucose oxidation. According to the cyclic voltammetric results and previous report (Jia et al., 2012), we elucidated the following mechanism of the glucose oxidation. After the oxidation of Ag_2O to AgO near 0.70 V in the anodic scan, glucolactone was formed through the reaction of AgO with glucose. As a result, the peak around 0.70 V increased significantly in the presence of glucose.

$$Ag_2O \rightarrow 2AgO + 2e^-$$

$$AgO + glucose \rightarrow Ag_2O + glucolactone$$

In addition, the effect of scan rate on the electrocatalytic oxidation of glucose at the LTA/GCE was investigated by cyclic voltammetry (Fig. 3.B). The scan rate was varied from 40 to 300 mV/s. Both the currents of anodic peak (0.70 V) and cathodic

peak (0.61 V) were proportional to the square root of the scan rate. These phenomena indicated that the oxidation of glucose by AgO is a diffusion-controlled process(Cao and Wang, 2010).

3.4. Optimization of glucose sensor performance

To further enhance the performance of the analytical system for glucose sensor, various factors influencing the response of the sensor, including the amount of LTA, the applied potential and the concentration of NaOH solution, were investigated. In order to understand the role of LTA content in the glucose oxidation, the current response of 1.0 mM glucose in 0.2 M NaOH solution was investigated. When the amount of LTA changed within the range of 1~8 mg mL^{-1}, the current response increased with the increasing amount of LTA from 1 to 3 mg mL^{-1} and decreased above 3 mg mL^{-1}. A possible reason for this is that an increase in the amount of redundant LTA decreased the electrode surface electroconductivity because of the semiconductive nature of perovskite. Therefore, the LTA content of 3 mg mL^{-1} was chosen in the following experiments.

It is important to select a suitable detection potential so as to obtain highly sensitive current response for glucose oxidation. The constant potential chronoamperometry was performed by varying the potential (in 0.05 V steps) of the LTA electrode between 0.6 and 0.8 V in the presence of 10 μM glucose (Fig. 4.A). The steady-state anodic current increases gradually with the increase of the potential. As a high potential would oxidize some interfering species that were stable under relatively low potential, +0.70 V was selected to suit our further research work.

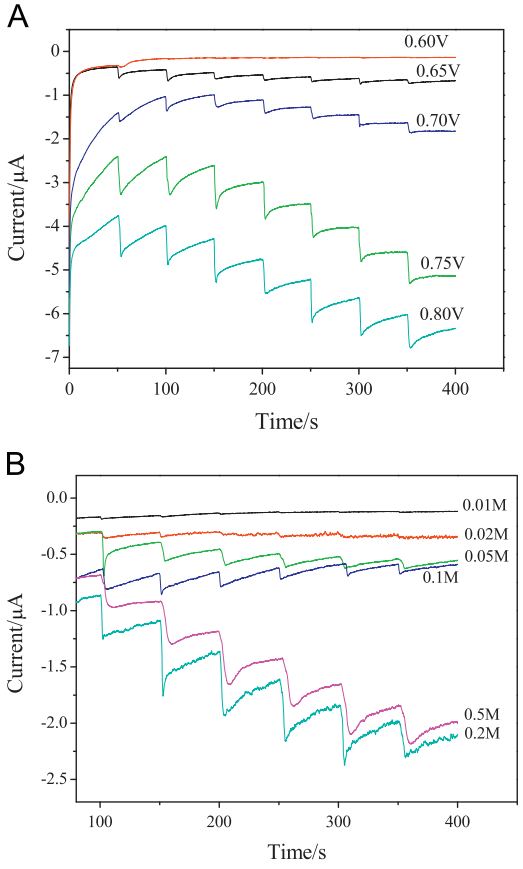

Fig. 4. Effect of applied potential on the amperometric response of the LTA/GCE to 10 μM glucose (A). The effect of the concentration of NaOH with 0.01 M, 0.02 M, 0.05 M, 0.1 M, 0.2 M and 0.5 M on the amperometric responses of 0.1 M glucose at the LTA/GCE (B).

An alkaline medium is normally required for enhancing the oxidation of carbohydrate compounds. Therefore, the effect of the concentration of NaOH on the amperometric responses of 0.1 M glucose at the LTA/GCE was examined using amperometric technique. As shown in Fig. 4B, when the concentration of NaOH solution changed from 0.01 to 0.2 M, the currents gradually increased, which is in constant with the fact that glucose is easily oxidized at higher pH. However, when the concentration of NaOH increased to above 0.2 M, the currents decreased, possibly due to the reason that too much OH^- can block the further electroadsorption of glucose anion (per glucose molecule lost one proton at about −0.12 V). Based on the above measurements, the optimal detection conditions of the modified electrode toward glucose can be summarized as: 3 mg mL^{-1} LNT, 0.7 V applied potential and 0.2 M NaOH solution.

3.5. Amperometric response and calibration curve of glucose

Based on the above-mentioned optimum conditions, amperometric determination of glucose was investigated. The electrode was tested in response to the successive addition of glucose solution with different concentrations into 0.2 M NaOH solution at the potential of +0.7 V. The corresponding results are shown in Fig. 5. When glucose was added into the NaOH solution, the current response of the LTA/GCE electrode changed very fast and reached a stable value quickly, and it achieved 95% of the steady-state current within 6 s.

The calibration curve for glucose detection at the LTA/GCE was investigated under optimal experimental conditions, and the results are given in Fig. 5. The linear range of the glucose sensor is from 2.5 μM to 4 mM (R=0.9997) with the corresponding linear equations I (μA)=7.4858 × 10^{-7}+0.00126C (M). The detection limit is 2.1 × 10^{-7} M and the sensitivity is 784.14 μA$M^{-1}cm^{-2}$. Although our detection limit is not lower than that of the references (Wang et al., 2010; Zhang et al., 2012), the sensors we construct have the advantages of strong anti-interference ability in high potential and can be used to detect real samples etc.

3.6. Interferences

Ascorbic acid (AA), dopamine (DA) and uric acid (UA) are co-existed with glucose in natural samples and these interfering species can normally produce the oxidation current comparable to that of glucose. To evaluate the selectivity of the new sensors, we investigated the amperometric responses of the LTA modified

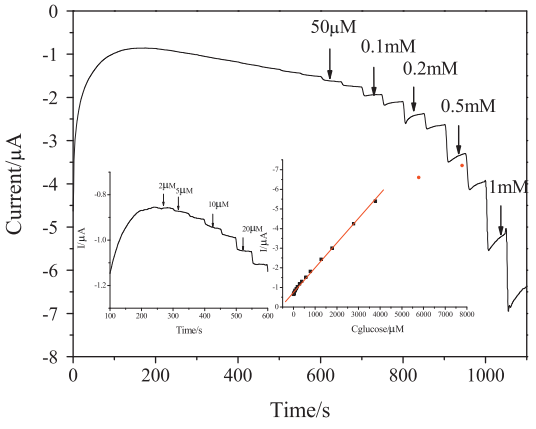

Fig. 5. Current–time responses of the LTA/GCE upon successive addition of different concentrations of glucose to NaOH solution under stirring condition. The applied potential was 0.7 V and the scan rate was 100 mV/s. The lower right inset presents the corresponding calibration curve response to the different concentration of glucose at the LTA/GCE in 0.2 M NaOH solution.

Table 1
Determination of glucose in human blood serum samples.

Serum samples	Hospital (mM)	Sensor (mM)	RSD (%)	Added (mM)	Recovery (%)
1	12.16	12.47	2.5	5	101.8
2	4.57	4.72	3.3	5	101.5
3	5.89	6.03	2.3	5	101.3
4	4.64	4.85	4.5	5	102.2
5	4.22	4.46	5.6	5	102.6

electrode at an applied potential of +0.7 V in 0.2 M NaOH solution with continuous additions of 1 mM glucose, 0.1 mM UA, 0.1 mM AA, 0.1 mM DA. (Because the blood glucose level of a normal human body is between 4 and 7 mM, while the concentration of endogenous AA and UA is about 0.125 mM and 0.33 mM, respectively (Song et al., 2005). Interestingly, it is observed that UA, AA and DA do not obviously perturb the detection of the glucose in its normal physiological level. The high selectivity is attributed to the structure of the perovskite LTA nanopaticles with higher real surface area; these accelerate the kinetically controlled sluggish reaction (the electrocatalytic oxidation of glucose) while the electro-oxidation of the interfering species are diffusion-controlled electrochemical processes but with a high steric hindrance by LTA coating on the electrode surface (Li et al., 2007). For a diffusion-controlled reaction, upon application of an anodic potential to the electrode, the surface concentration of the reactant will be immediately depleted to zero; therefore, a concentration gradient of the reactant near the electrode surface is established. Such a concentration gradient is called diffusion layer and has a range of a few micrometers. It will be formed in milliseconds due to electrode reaction and reactants inside the perovskite will be immediately depleted. As a result, the Faradic currents of the reactants are proportional to the apparent geometric area of the electrode, regardless of the perovskite roughness of the electrode (Yuan et al., 2005). Therefore, the LTA electrode is promising for the selective and sensitive detection of glucose.

3.7. Blood serum sample measurement

In order to discriminate whether there is matrix effect of blood on the prepared sensor, it was applied to determine glucose in blood serum samples (other parameters were used as optimum conditions), which were obtained from Huai'an First People's Hospital. It should be noted that, prior to use, the serum samples were diluted 100-fold with normal saline. Amperometric detection was applied at a given potential of 0.7 V in 10 mL 0.2 M NaOH solution with 10 μL blood serum injected. The quantitative determination of blood serum samples were carried out by using the standard addition method and the results were shown in Table 1. The tested results of the blood serum samples are in accordance with those determined by hospital, and recovery values are in the range of 101.3~102.6 (± 5%) as shown in Table 1, indicating that this method is reliable for the determination of glucose in real human serum.

3.8. Stability and reproducibility study

The stability of the LTA catalyst toward glucose oxidation was also studied. The electrode was tested in 0.2 M NaOH solution containing 0.1 mM glucose for 30 successive cyclic scans, and the CV curves remain almost the same, suggesting excellent stability of the modified electrode.

Furthermore, the concerning reproducibility of the sensor was evaluated by CVs. The relative standard deviation (RSD) of current signal for 0.1 mM glucose for 15 repeated measurements with the same perovskite LTA modified GCE was 3.57%. These results indicate that the proposed sensor has excellent reproducibility.

The long-term stability of the sensor was also examined in this work. When the sensor was stored at room temperature for a month, the amperometric current response was approximately 92% of its original counterpart.

4. Conclusion

A novel glucose electrochemical sensor based on perovskite LTA modified GCE was reported. LTA modified GCE showed high electrocatalytic activity for the glucose electrooxidation, and it could be used for sensitive detection of glucose. Compared with previous reports on similar nonenzymatic glucose sensors, this sensor showed lower detection limit, higher sensitivity, and much wider linear range. Moreover, the prepared sensor can be used for the detection of glucose in real samples with good accuracy. It is expected that this sensor, based on the novel perovskite-type oxide material, may find practical applications in the future for the assay of blood glucose.

Acknowledgments

This research is supported by the National Natural Science Foundation of China (20975043, 21073093, 51106061), Jiangsu Higher Institutions Key Basic Research Projects of Natural Science (09KJA530001, 10KJA430005) and the “Qinglan” Project of Jiangsu Province (2010).

References

Bohnke, O., Bohnke, C., Duroy, H., 2001. Chemistry of Materials 13, 1593–1599.
Cao, X., Wang, N., 2010. Electrochemistry Communications 12, 1581–1584.
Clark, L.C., Lyons, C., 1962. Annals of the New York Academy of Sciences 102, 29–45.
DeMott Jr, J.M., Jahngen, E.G.E., 2005. Electroanalysis 17, 599–606.
Ding, Y., Liu, Y.X., Parisi, J., Zhang, L.C., Lei, Y., 2011. Biosensors and Bioelectronics 28, 393–398.
Gu, H.Y., Yu, A.M., Chen, H.Y., 2001. Electroanalytical Chemistry 516, 119–126.
Jia, M.Z., Wang, T., Liang, F.F., Hu, J.B., 2012. Electroanalysis 24, 1864–1868.
Jiang, L.C., Zhang, W.D., 2010. Biosensors and Bioelectronics 25, 1402–1407.
Li, Y., Song, Y.Y., Yang, C., Xia, X.H., 2007. Electrochemistry Communications 9, 981–988.
Lin, C.Y., Lai, Y.H., Balamurugan, A., Vittal, R., Lin, C.W., Ho, K.C., 2010. Talanta 82, 340–347.
Lu, L.M., Zhang, L., Qu, F.L., Lu, H.X., Zhang, X.B., Wu, Z.S., 2009. Biosensors and Bioelectronics 25, 218–223.
Lu, L.M., Li, H.B., Qu, F., Zhang, X.B., Shen, G.L., Yu, R.Q., 2011. Biosensors and Bioelectronics 26, 3500–3504.
Lu, L.M., Zhang, X.B., Shen, G.L., Yu, R.Q., 2012. Analytica Chimica Acta 715, 99–104.
Pang, H., Lu, Q.Y., Wang, J.J., Li, Y.C., Gao, F., 2010. Chemical Communications 46, 2010–2012.
Song, Y.Y., Zhang, D., Gao, W., Xia, X.H., 2005. Chemistry—A European Journal 11, 2177–2182.
Sumio, K., Masataka, O., Mikio, S., 2004. Catalysis Surveys from Asia8 (l), 27–34.
Wang, B.J., Gu, S.Q., Ding, Y.P., Chu, Y.L., Zhang, Z., Ba, X., Zhang, Q.L., Li, X.R., 2013. Analyst 138, 362–367.
Wang, Y.L., Xu, Y.H., Luo, L.Q., Ding, Y.P., Liu, X.J., Huang, A.Q., 2010. Sensors and Actuators B 151, 65–70.
Wilson, R., Turner, A.P.F., 1992. Biosensors and Bioelectronics 7, 165–185.
Ye, D.X., Xu, Y.H., Luo, L.Q., Ding, Y.P., Wang, Y.L., Li, X.J., Xing, L.J., Peng, J.W., 2012. Colloids and Surfaces B 89, 10–14.
Yuan, J.H., Wang, K., Xia, X.H., 2005. Advanced Functional Materials 15, 803–809.
Zhang, Z., Gu, S.Q., Ding, Y.P., Jin, J.D., 2012. Analytica Chimica Acta 745, 112–117.
Zhu, L.D., Tian, C.Y., Yang, D.X., Jiang, X.Y., Yang, R.L., 2008. Electroanalysis 20, 2518–2525.
Zhu, X.L., Gan, X., Wang, J., Chen, T., Li, G.X., 2005. Journal of Molecular Catalysis A: Chemical 239, 201–204.